Linking hydrogeomorphological diversity to biodiversity and functioning in running waters

Christine Anlanger[1,2]* (0000-0001-6666-422X), Christian Noss[1,3] (0000-0003-4150-5868), Ute Risse-Buhl[1,2] (0000-0002-7219-5172), Mario Brauns[2] (0000-0002-5012-9721), Daniel von Schiller[4,5] (0000-0002-9493-3244), Markus Weitere[2] (0000-0002-5259-2293) and Andreas Lorke[1] (0000-0001-5533-1817)

[1]Institute for Environmental Sciences, University of Kaiserslautern-Landau, Fortstrasse 7, 76829 Landau, Germany

[2]Department of River Ecology, Helmholtz Centre for Environmental Research – UFZ, Brueckstrasse 3a, 39114 Magdeburg, Germany

[3]Federal Waterways Engineering and Research Institute, Kussmaulstrasse 17, 76187 Karlsruhe, Germany

[4]Departament de Biologia Evolutiva, Ecologia i Ciències Ambientals (BEECA), Universitat de Barcelona (UB), Av. Diagonal 643, 08028 Barcelona, Spain

[5]Institut de Recerca de l'Aigua (IdRA), C/Montalegre 6, 08001 Barcelona, Spain

Running head: Hydrogeomorphological effects on biodiversity and functioning

Keywords: flow, turbulence, streambed topography, biofilms, bacteria, autotrophs, phagotrophic protists, nitrogen uptake, ecological niches

Authors' contribution: Conception and design of the work: CA, CN, URB, MW, AL; Data acquisition: CA, CN; Data analysis and interpretation: all authors; Drafted the work and wrote

the manuscript: CA, AL with the help of CN, URB, MW, MB, DvS; all authors helped to revise the work and approved the final submitted manuscript.

Abstract

Hydrogeomorphological diversity is supposed to be an important driver of the biodiversity and functioning of running waters. Experimental evidence, however, has been restricted to selected spatial and temporal scales. Here, we present a framework for quantifying hydrogeomorphological diversity based on additive variance partitioning similar to established biological concepts based on α, β and γ diversities. By testing this framework with empirical data from streams, we demonstrate that the spatial flow variability (flow β diversity) is the prime driver of the β diversity of biofilm-dwelling autotrophs and phagotrophic protists as well as nitrogen uptake efficiency, thereby underlining the relevance of hydrogeomorphological niches. Our framework facilitates the joint analysis of the interaction among hydrogeomorphology, biodiversity and ecosystem functioning. Furthermore, our framework can guide hydroecological research by integrating it into a broadened diversity concept and help optimizing hydrogeomorphological restoration measures to recover the structure and functioning of running waters.

Introduction

Environmental heterogeneity induced by physical and biotic factors is a major attribute of ecosystems and can be defined as the variability in processes or patterns over space and time[1,2]. The habitat heterogeneity hypothesis postulates that species diversity increases with environmental heterogeneity because more complex habitats provide more niches and a more diverse supply of resources[3]. Increased habitat heterogeneity should thus increase the ability

of ecosystems to maintain their functionality despite temporal variations in environmental conditions[4].

In streams and rivers, habitat heterogeneity is commonly related to the spatial and temporal variability of hydrogeomorphology considered in terms of stream flow velocity and streambed geomorphology[5,6]. Streambed roughness has been shown to affect the hydraulic habitat and mixing processes at the benthic interface[7,8]. Spatially, habitats are structured hierarchically and extend from microhabitats (for biofilm communities as considered here ~ 10^{-2}–10^{-1}m, hereafter referred to as spots), mesohabitats (10^{0} m) to reaches (~ 10^{1}–10^{2} m), segments (~ 10^{2} m) and catchments (~ 10^{3} m), with mutual interactions among habitats[9,10]. Temporal variations of flow velocities range from milliseconds to minutes (i.e., the hydraulic scale of velocity fluctuations) up to days, months and years (i.e., the hydrologic scale of flow fluctuations[6]).

Most empirical studies in running waters have used bulk measures of hydrogeomorphological parameters (e.g., mean flow velocity, water depth, wetted area, and bed slope) to characterize spatial habitat heterogeneity[11–15], and only a few linked habitat heterogeneity to biological communities at identical scales[16–18]. Moreover, empirical assessments of biogeochemical cycling and water quality in streams are typically conducted at the reach or larger spatial scales[15,19]. Yet, reach-scale properties emerge from strongly varying smaller-scale hydrogeomorphological conditions, which need to be considered for extrapolation to larger spatial scales[2,16]. Furthermore, temporal variations of flow velocity have rarely been considered for characterizing heterogeneity at the micro scale[17,21], even though high-frequency turbulent velocity fluctuations affect the structure and functioning of surface-associated microbial communities (biofilms) in streams[16,22].

Yet, the broad range of hydrogeomorphological diversity that potentially affects the biodiversity and functioning of running waters has not been addressed so far. This is urgently

needed to improve our understanding of how hydrogeomorphological dynamics across different spatial and temporal scales shape the biodiversity and functioning of these ecosystems[23,24]. Moreover, planning and successful implementation of restoration efforts require a scalable framework to characterize the habitat heterogeneity needed to restore biodiversity and ecosystem functions to natural levels.

Here, we describe a novel framework for characterizing habitat heterogeneity in running waters by a diversity index that combines measures of spatial and temporal variability of hydrogeomorphology across different scales by variance partitioning. Variance partitioning has been used in geographical analyses for almost half a century[25]; it has been widely applied in various fields, including landscape ecology[26] and river science[27,28], but has rarely been connected to habitat heterogeneity, biodiversity and ecological functioning. We adopt this framework to quantify relationships between hydrogeomorphological diversity and biofilm diversity, including bacteria, autotrophs and phagotrophic protists, representing the key guilds of biofilm food webs in running waters[29]. Moreover, we link hydrogeomorphological diversity to stream functioning quantified as areal nitrogen uptake. In doing so, we aim to identify the relevant scales at which flow and geomorphological diversity of the streambed are interacting and at what scales flow diversity affects biodiversity and the diversity of biogeochemical hot spots.

Results and Discussion

Conceptual framework of hydrogeomorphological diversity

The scale-dependence of biotic diversity is commonly characterized by alpha (α), beta (β) and gamma (γ) diversities[30,31]. The α diversity describes the number of species (i.e., species richness) or species diversity at a particular spot, i.e. at micro scale. The β diversity represents

93 the change in species richness or diversity between spots, while the γ diversity refers to the
94 overall species richness or diversity of all spots within a region (Fig. 1a). Partitioning the
95 overall diversity into α and β components should fulfill several basic properties. Among these
96 are the requirements that α and β diversity should vary independently and that γ diversity
97 should be completely determined by α and β diversities[32]. The latter can be achieved through
98 either an additive or a multiplicative approach between both diversities[33]. The additive
99 approach offers the advantage of direct comparability between diversities, as they are
100 expressed in the same unit.

101 Similar to biodiversity partitioning, we applied an additive approach to characterize
102 the hydrogeomorphological diversity of running waters (Fig. 1b-d). Generally, α diversity
103 represents the normalized variance of a hydrogeomorphological measure (e.g., flow velocity
104 or water depth) at a particular spot. Similarly, we express γ diversity as the normalized
105 variance of a hydrogeomorphological measure at different spots within a larger spatial scale.
106 Finally, β diversity, representing the spatial variance of the mean values, is obtained from the
107 additive definition of diversities as $\beta = \gamma - \langle a \rangle$, with $\langle a \rangle$ representing the mean value of all
108 α diversities observed at the corresponding scale. The normalization of the variances avoids
109 inherent dependencies between variance and mean values, which are known to exist for many
110 physical quantities, including flow velocity[34].

111 The flow diversities should integrate temporal fluctuations (characterizing local
112 turbulence) and spatial flow variability because both are important characteristics defining
113 habitat suitability and ecological patterns in running waters across various scales[35,36].
114 Therefore, flow α diversity at individual spots is calculated as the variance of temporal
115 velocity fluctuations normalized by the mean flow velocity squared. This quantity
116 corresponds to the square of the turbulence intensity[37] (i.e., the twofold ratio of turbulent
117 kinetic energy and squared mean flow velocity). It should be noted that in homogeneous

boundary-layer flows, the turbulent kinetic energy is linearly related to the square of the mean flow velocity. Hence, spatial variations in flow α diversity do not reflect different magnitudes in turbulent kinetic energy, but rather different qualities of turbulence, e.g. different eddy sizes, that result in different relationships between turbulent kinetic energy and mean flow velocity. Flow β diversity describes the spatial variability of mean (time-averaged) flow velocities and is normalized by the square of the overall mean velocity at larger scales (meso scale or reach scale). This quantity has been used in several models (e.g., *Mesohabitat Evaluation Model*[38], *Mesohabitat Simulation Model*[39]) or as an index to describe habitat preferences of biotic communities[11]. Finally, flow γ diversity represents the total velocity variance, including the spatial variance of mean flow velocity (β) and the mean turbulent intensities (Fig. 1, see also the Methods section for details on the calculation of flow diversities).

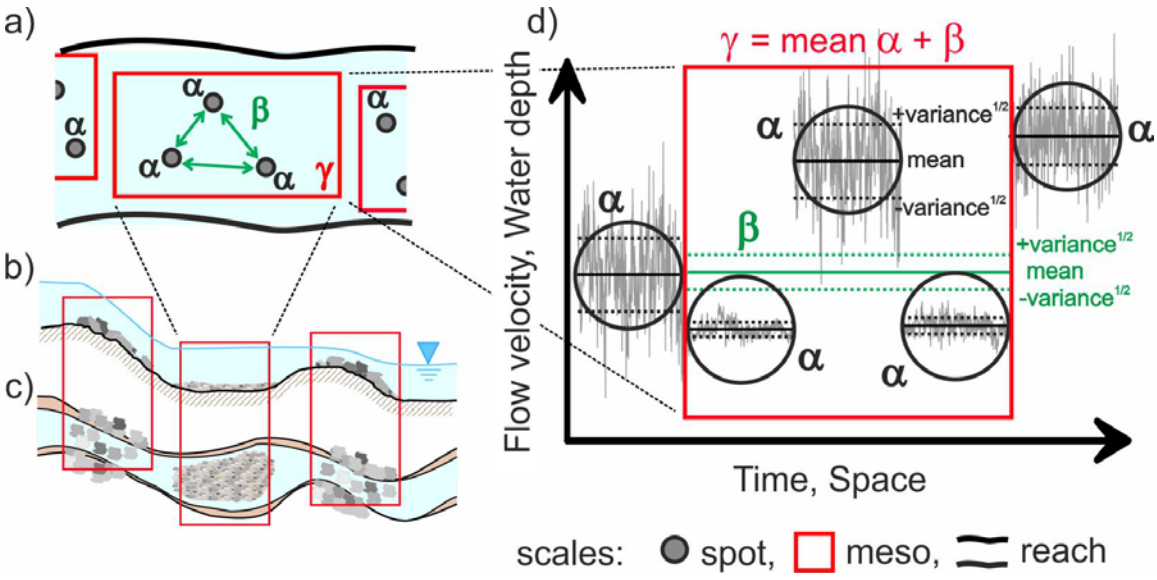

Figure 1. Framework for quantifying hydrogeomorphological diversity in streams across spatial and temporal scales. The framework is based on additive variance partitioning similar to established biological concepts. It describes hydrogeomorphological diversity at individual spots (α diversity), between spots (β diversity, green arrow) and the overall diversity within a larger region (γ diversity (a)). The α diversity describes the variance of flow velocity or water depth measured at individual spots, and γ diversity is the total variance observed at larger scales. Larger scales include riffles and pools at the meso scale or the reach scale (schematic longitudinal transect (b) and plan view (c)). β diversity measures the difference in diversities between spots and, using an additive approach, represents the variability of mean values at a smaller scale within a larger scale (d). β and γ diversities are shown for the meso scale only. However, the diversities can also be calculated for the reach scale, with β diversity expressing the variation between meso habitats and γ diversity expressing the overall diversity of the reach.

Geomorphological diversity describes spatial variations in streambed elevation, commonly decomposed into different types of roughness (e.g., grain roughness) and bed slope or larger-scale topography[40]. Geomorphological α diversity is calculated as the variance of water depths normalized by the squared mean water depth at the spot (Fig. 1), equivalent to the square of the relative streambed roughness and the reciprocal of the squared relative submergence [40,41]. At the meso or reach scale, geomorphological γ diversity describes the variance of local water depths normalized by the square of the mean water depth at larger scales, and we refer to it as overall geomorphological diversity. Finally, the geomorphological β diversity is the variability of the mean water depths at the spot scale normalized by the squared mean water depth (Table 1 in Methods).

Variance partitioning of physical quantities is not new in fluvial hydraulics, and flow velocities measured at one particular spot are often decomposed into mean values, which vary with discharge and location, and high-frequency turbulent velocity fluctuations (Reynolds

144 decomposition[6]). The double-averaging approach additionally takes spatial variations of flow
145 properties into account[42–44].

146 In this study, we applied the framework to measurements of flow velocity and water
147 depth, at spatiotemporal scales relevant to biofilm diversity and functioning in gravel-bed
148 streams. Given the universality of the underlying variance partitioning, the framework can be
149 applied to ecosystems and communities beyond biofilms in running waters. For example, it
150 can be used to quantify effects of hydrogeomorphology on the diversity of larger-sized and
151 motile organisms, such as macroinvertebrates or fish, given that flow diversity has been
152 recognized as an important physical control on their community composition[12,45,46]. In larger
153 lowland rivers, the hydrogeomorphological α and β diversities can be used to study their
154 effects on planktonic algae[47]. However, for studies on ecological and biogeochemical
155 processes in the hyporheic zone, and for assessments of whole-stream functioning and
156 diversities, additional hydrogeomorphological variables that relate to hyporheic exchange
157 rates can become more relevant and the characterization of the morphological diversity needs
158 to be extended accordingly.

159 We applied the concept to running waters, where normalization of variances by mean
160 quantities was important to avoid inherent dependencies between turbulence and mean flow,
161 i.e. between alpha and beta diversities. Besides smaller modifications concerning the
162 normalization, the concept can also be applied to lentic ecosystems, such as lakes, wetlands
163 and impoundments. For example, flow diversity could be analyzed within different lake
164 habitats (e.g., littoral versus benthic, and pelagic zones), as well as across lakes to explain
165 patterns and differences in algal bloom formation, for which flow and turbulence are
166 important drivers[48,49]. Generally, the variance partitioning approach can be readily applied to
167 other abiotic variables, such as light, temperature, resource and pollutant concentrations, for
168 linking these to biological variables at commensurate scales. The diversity measures can

169 therefore be applied for quantitative assessments of ecological consequences of changing
170 stream temperature[50,51], as well as to assess the spatial and temporal variations in chemical
171 exposure to toxicants[52].

172 **Application of the diversity framework**

173 Our proposed framework was applied to an existing data set of high-frequency
174 measurements of near-bed flow velocities conducted at the spot scale (10^{-2} m) at two seasons
175 in two gravel bed streams with different nutrient backgrounds[16,22,53]. The selected study
176 reaches (588 m and 510 m long) exhibited natural flow regimes with base flow discharge of
177 0.18 $m^3 s^{-1}$ and 0.24 $m^3 s^{-1}$, mean water level slopes of 0.82% and 0.39%, and mean stream
178 widths of 7.2 m and 7.3 m, respectively. Flow measurements were accompanied by
179 measurements of the streambed topography in 1x1 m patches along the reaches and were used
180 to quantify geomorphological diversity (see method section for details on topographic
181 measurements). The existing data also included microbial species richness in biofilms, which
182 was estimated in samples collected shortly after the flow velocity measurements at identical
183 spatial scales (i.e., spot scale, 10^{-2} m) and analyzed using both microscopic and molecular
184 approaches[16]. We quantified ecosystem functioning as areal nitrogen uptake of biofilms,
185 which was available from previously analyzed experiments at the study reaches, which
186 included whole-stream additions of ^{15}N-labelled ammonium chloride for 24 h periods and
187 subsequent biofilm sampling[53,54]. A nested sampling design expanded the spot (i.e., micro
188 scale) to the meso and the reach scale (Fig. S2 in Supplement). The α and γ diversity of each
189 microbial guild was expressed as species richness. The α and γ diversity of areal nitrogen
190 uptake rates and uptake efficiencies were expressed as the coefficient of variation. Following
191 our conceptual framework of hydrogeomorphological diversity, β diversities were calculated
192 by subtracting mean α diversity from γ diversity. We used linear models to relate the

diversities of streambed geomorphology, microbial guilds and areal nitrogen uptake to flow diversity and found a significant positive relationship in 12 out of 18 models (Fig. 2). The β and γ flow diversity increased with β and γ biodiversity and β and γ diversity of nitrogen uptake efficiencies. In contrast, flow diversity was unrelated to the mean α diversity of microbial guilds, and areal nitrogen uptake rates and efficiencies, but significantly related to season and stream.

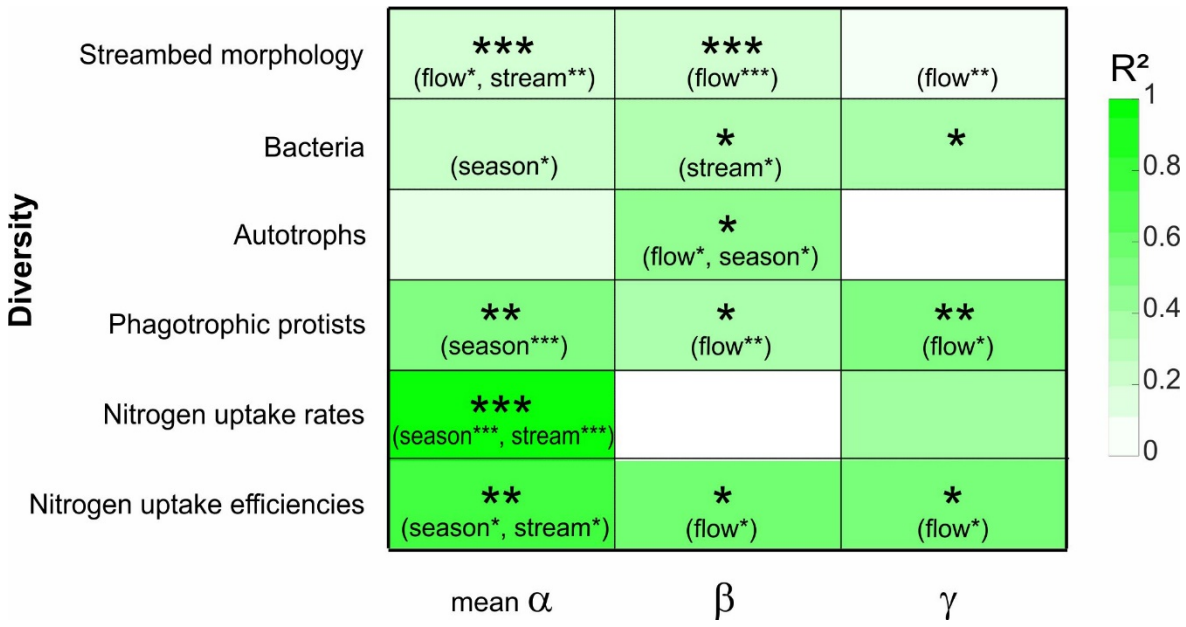

Figure 2. Heatplot visualizing the proportion of variance of different diversities explained by the flow mean α, β and γ diversity (columns), season and stream. The response variables are the geomorphological mean α, β and γ diversity of the streambed, the mean α, β and γ diversity of microbial guilds (TR-Fs of prokaryotic 16S rRNA genes abbreviated as bacteria, autotrophic morphotypes abbreviated as autotrophs and phagotrophic protist morphotypes abbreviated as phagotrophic protists), and the mean α, β and γ diversity of areal nitrogen uptake rates and efficiencies. Bold stars show the level of significance of the individual models, and the text followed by small stars shows the significance of the explanatory variables ($p < 0.05$ *, $p < 0.01$ **, $p < 0.001$ ***).

Flow and geomorphological diversities

The mean overall diversities (γ diversities) of flow and streambed geomorphology increased with increasing spatial scale, mainly due to increased mean spatial variability (β

202 diversities). In contrast, the mean temporal flow variability (flow α diversity, corresponding
203 to turbulence intensity) and streambed roughness (geomorphological α diversity) increased
204 only slightly or were nearly constant across both scales (Fig. 3a). The mean flow velocity
205 varied stronger between larger-scale features of the stream bed (i.e., pool-riffle structures at
206 the meso scale) than due to small-scale streambed roughness. This result agrees with previous
207 findings that water depth affects turbulent flow structures more than protruding streambed
208 elements[8]. The strong increase in geomorphological β and γ diversities from the meso to the
209 reach scale in our study was associated with changes in the bulk geometry of the streambed,
210 in addition to the predominant effect of form roughness at smaller scales. Here, the highest
211 relative contributions of β diversity to γ diversity were obvious for geomorphological
212 diversity and accounted for 77% and 95% at the meso and reach scale, respectively (Fig 3a).

213 We found a strong relationship between flow and geomorphological β diversities
214 ($F_{1,69} = 21.64$, $p < 0.001$, Fig. 2), which was expected given that the mean flow velocity
215 depends strongly on the relative submergence of the streambed. Previous studies have found a
216 wide range of power law-relationships between relative submergence and mean flow or vice
217 versa between relative roughness and flow resistance[55]. Skin friction dominates the resistance
218 force at high relative submergence and depends only weakly on the relative roughness
219 (approximately with the power of 1/6). At lower relative submergence, as in the present study,
220 larger contributions from form drag forces resulted in a nearly linear relationship between
221 flow resistance and relative roughness. Similar results were found in sandy lowland streams[7],
222 highlighting the universality of this relationship for other stream types. The relationship
223 between the relative submergence at the grain scale (geomorphological mean α diversity) and
224 temporal flow variability (flow mean α diversity) differed among streams (Fig. 2), which may
225 result from differences in bed slope[54] and roughness between stream reaches (Fig. S1 in the

Supplement). Seasonal differences were not relevant for any relationships between flow and geomorphology because of lacking bed-forming discharges during the study.

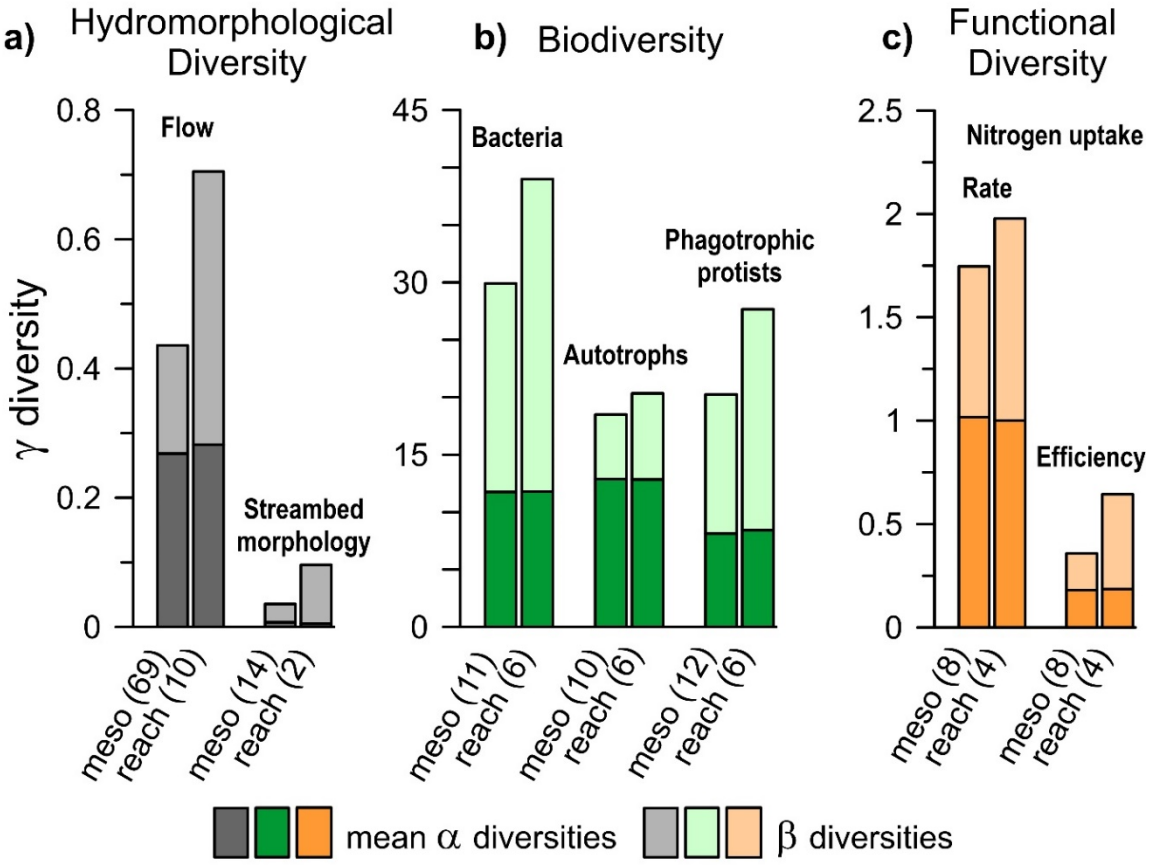

Figure 3. Mean contributions of mean α and β diversities to γ diversity of (a) hydrogeomorphological diversity (flow and streambed geomorphology), (b) biodiversity including three microbial guilds (T-RFs of prokaryotic 16S rRNA genes abbreviated as bacteria, autotrophic morphotypes abbreviated as autotrophs, phagotrophic protist morphotypes abbreviated as phagotrophic protists), and (c) the diversity of areal nitrogen uptake rates and efficiencies as proxies for ecosystem functioning. Data for each scale and diversity are averaged over all seasons and streams, where the number of data points is shown in parentheses in the axis labels.

Flow diversity and biodiversity

Turbulence intensity (flow α diversity) did not significantly affect any diversity of microbial guilds (Fig. 2), demonstrating that species richness can be equally high over a wide range of natural flow variability. However, species identity might still be affected by shifts in

232 species differing in their tolerance towards hydraulic forces (see Risse-Buhl et al.,[16] for more
233 detailed community analyses). By contrast, spatial (β) flow diversity significantly affected β
234 diversity of autotrophs ($F_{1,12}$ = 6.13, p = 0.029) and phagotrophic protists ($F_{1,14}$ = 11.55,
235 p = 0.004). The latter was also significantly affected by the overall flow diversity, combining
236 both turbulence intensity and spatial variability of the mean flow (flow γ diversity, $F_{1,14}$ =
237 16.04, p = 0.001, Fig. 2). Following the hydrogeomorphological diversities, the γ diversity of
238 the studied microbial guilds increased with spatial scale due to an increase in β diversities.
239 This result followed the prediction of the dual scaling law that states that species richness
240 increases with increasing spatial scale and environmental heterogeneity[56].

241 Contrary to bacteria and phagotrophic protists, the overall diversity of autotrophs (γ
242 diversity) showed higher contributions of the mean α diversity, which was similarly high for
243 both spatial scales (69% and 63% for the meso and reach scale, respectively, Fig. 3b). The
244 overall diversity of autotrophs was high already at the small scales, which implies that flow
245 variability induced by riffle-pool sequences is of minor importance at least for the
246 morphotype diversity of this microbial guild. The autotrophic community that developed
247 during biofilm maturation can act as an ecosystem engineer, which might results in a
248 homogenization of communities between spot scales by modulating their microenvironment
249 and creating similar biofilm architectures and flow conditions[57].

250 Bacterial diversity did not respond to flow diversity, whereas flow diversity at larger
251 scales affected the diversity of autotrophs and phagotrophic protists. Phagotrophic protists
252 and most autotrophs are relatively large (compared to bacteria) and show a large phenotypic
253 diversity with diverse adaptations to flow and corresponding preference for particular
254 hydraulic niches[58–60]. This makes the sorting of species by hydraulic forces likely. In contrast
255 to phagotrophic protists, the dominant bacterial species occurred irrespective of the turbulent
256 kinetic energy at the spot scale[16]. Here, we confirm this finding also for the flow diversities at

larger spatial scales. The lifestyle of bacteria is characterized by smaller organismic size, high production of protecting and fixing extracellular polymeric substances[61,62], and a high phenological plasticity[63]. All these features make them highly ubiquitous and resistant to physical forcing in the stream environment. The high phenotypic plasticity of bacterial genotypes potentially enables the same genotype to occur with adapted phenotypes in different hydraulic niches. However, the high contribution of β diversity to the overall γ diversity (Fig. 3) suggests a differentiation and the existence of distinct communities at different spots, which were unrelated to flow diversity (Fig. 2). It is important to note that the bacteria were analyzed using molecular methods based on 16S rRNA genes. In contrast, autotrophs and phagotrophic protists were microscopically counted based on phenotypic and morphological features (see methods). As habitat adaptation occurs at the phenotype level and particularly bacteria show extremely high phenotypic plasticity within particular genotypes, the phenotypic bacterial diversity may show different patterns compared to the genotypic diversity analysed here.

In agreement with previous results[16], the mean α diversities of bacteria ($F_{1,13} = 4.90$, $p = 0.045$) and phagotrophic protists ($F_{1,14} = 16.98$, $p = 0.001$) were significantly affected by season (Fig. 2), indicating that the variability in environmental conditions (e.g., nutrients, light, temperature, the seasonal succession of predators and prey) constrained biofilms along the whole stream reach (i.e., large-scale effects).

Flow and functional diversity

Mean α and β diversities of the nitrogen uptake efficiency at the meso scale contributed equally to its γ diversity (Fig. 3c), implying that the variability of nitrogen uptake efficiency within individual riffle and pool structures was comparable to the variability between structures of the same type. For areal nitrogen uptake rates, the mean α diversity was slightly

281 higher than the β diversity (58% and 42% of the γ diversity, respectively). At the reach scale,
282 the β diversity of nitrogen uptake efficiencies was 2.5 times larger than the corresponding
283 mean α diversity. However, both diversities were similar for areal nitrogen uptake rates (Fig.
284 3c). As the uptake efficiency corresponds to the biomass-specific uptake rate, this finding
285 suggests that the conditioning of biomass within and between meso scale structures supports
286 similar, i.e. less diverse, uptake rates despite different flow conditions.

287 Turbulence intensity (flow α diversity) had no significant effect on the diversity of
288 nitrogen uptake rates or nitrogen uptake efficiencies (Fig. 2). However, we found that the
289 spatial variability of the mean flow velocity (flow β diversity) influenced the β diversity of
290 the nitrogen uptake efficiency ($F_{1,8}$ = 10.69, p = 0.011) and the overall (γ) flow diversity
291 influenced the γ diversity of nitrogen uptake efficiency ($F_{1,8}$ = 8.78, p = 0.018). The lack of
292 influence of spatial variations in flow α diversity on nitrogen uptake efficiencies appears
293 surprising, as the maximum rate at which biofilms can take up nitrogen from the stream water
294 is limited by turbulent mass transfer at the streambed[64]. While previous analysis of the same
295 data demonstrated that nitrogen uptake efficiencies in the studied streams increased with
296 increasing near-bed turbulence following a universal scaling relationship[53], this relationship is
297 removed by the normalization of alpha diversities with the square of the mean flow velocity.
298 Spatial variations in flow α diversity, which represent different relationships between
299 turbulent kinetic energy and mean flow velocity due to different streambed roughness, were
300 small when comparing pools and riffles. The spatial variability in turbulent kinetic energy,
301 which results from variations in mean flow velocity, is therefore represented by the flow β
302 diversity, which was positively related to the observed nitrogen uptake efficiencies in
303 accordance with the previous studies.

304 To analyze whether the effects of flow on nitrogen uptake diversity are mediated by
305 relationships between biodiversity and functional diversity, we related the diversity of

306 individual microbial guilds to the diversity of the areal nitrogen uptake rate and uptake
307 efficiency, while considering stream and season as additional explanatory variables.
308 Diversities of autotrophs were not significantly correlated to the diversities of nitrogen uptake
309 rates or efficiencies (Fig. S3-S5). However, the spatial variability of the mean flow was
310 correlated with both the β diversities of autotrophs (see previous section, Fig. 2) and the
311 nitrogen uptake efficiency (Fig. 2). As described above, autotrophs exhibited high α and low
312 β diversities (Fig. 3b), suggesting that the effects of flow diversity on the diversity of nutrient
313 uptake were unrelated to the identity of particular microbial species, but rather to their
314 functional performance.

315 Our approach to quantifying the diversity of a single function diverges from the
316 common approach to measure the diversity of multiple functions, known as
317 multifunctionality. Nevertheless, our approach highlights that ecosystem functions are not
318 homogenously distributed over space, and there are communities within stream reaches with a
319 higher contribution to whole-ecosystem function than others. We demonstrated that a
320 significant part of this variation is driven by habitat heterogeneity, quantified as flow
321 β diversity. Predicting the location of those functional hotspots based on measures of
322 hydrogeomorphological diversity is a promising avenue for future research. From a
323 methodological point of view, our results are also important for designing whole-stream
324 uptake studies that usually sample a few spots to characterize whole-ecosystem function.
325 Knowing where functional hotspots are located may help to prevent undersampling the true
326 functional variation and avoid erroneous estimates of whole-ecosystem functioning.

327 Contrarily, the mean areal nitrogen uptake rate and efficiency (not their diversity) were
328 not related to α, β or γ diversities of different microbial guilds except for the mean α diversity
329 of bacteria (Fig. S6-S7). This is not surprising given the effects of flow diversity on the
330 diversity of the nitrogen uptake. This finding also contradicts laboratory studies with

heterogeneous flows[60], where nitrogen uptake increased with species richness in algal biofilm communities due to niche partitioning. These contrasting results may be due to large differences in species richness between this particular laboratory experiments with a maximum number of 8 species, and natural ecosystems, where functional redundancy and dominance effects become important[65,66].

Temporal and spatial upscaling

Upscaling of measurements in space and time is of great importance in ecology and biogeography[20,67]. Furthermore, integration of events over time can be essential to explain current patterns. Specifically, the species composition, abundance and morphology of biofilms can be influenced by flow conditions during the last days or weeks.

The cumulative integral of the geomorphological α diversity of the streambed, which was derived from cross-sectional transects available for 13 km of one of the study streams, indicates that the geomorphological diversity strongly increased at scales larger than the meso scale (Fig. S8b). Geomorphological diversity associated with riffles and pools at the meso scale contributed <10%, while the highest diversity was observed at spatial scales between 100 m and ~2 km, which is similar to the reach scale and confirms the choice of this upper scale in the empirical studies from which the data were adopted.

All sampling was conducted at nearly stationary discharge conditions that persisted for at least two weeks before each sampling, and discharge magnitude was comparable between samplings. Thus, the estimated flow α diversities include only the hydraulic scales of velocity variance (turbulence intensity) but not the hydrological scales of flow variability. The specific definition of the flow α diversity applied here allows for an easy extension of the concept to include also longer-term temporal flow variations derived from long-term discharge monitoring at both streams. By analyzing the cumulative integral of the power spectrum of

the temporal flow variability (i.e., flow α diversities) derived from long-term discharge time series, we found that the flow α diversity resolved in the measurements contributed, on average only 20% to the long-term flow α diversity over 16 years (Fig. S8a). This contribution varied between 2% and 70%, depending on the sampling spot. Most contributions to the long-term flow α diversities were associated with seasonal discharge variations at annual time scales. Discharge-related variations in mean flow velocity will not necessarily translate into variations in turbulence intensity due to the inherent relationship between turbulent kinetic energy and mean flow velocity. Instead, the low-frequency temporal flow variability would rather result in different magnitudes and spatial arrangements of mean flow velocities, and thus have similar effects on biofilms as the flow β diversity in our analysis. However, biofilm communities and functions vary with season in response to other environmental constraints and we expect that diversities and their interrelations may change with time. Furthermore, increasing drag forces and transport of suspended matter during repeating high-discharge events at hydrological scales can temporarily reduce biofilm biomass[68] and eventually these hydrological variations might overrule/mask the effects of season and stream at the scales investigated here.

The integration of temporal and spatial scales in diversity assessments remains a challenging task, not only in ecology. Specifically, integration over time is still missing in global assessments of human impact on freshwater biodiversity[69]. Our data do not allow predictions of how changes in temporal flow diversity might affect spatial and temporal components of biodiversity and the diversity of functions. Therefore, we advocate for future studies that should involve sampling of biotic and functional diversities over a range of spatial and temporal scales. The framework presented here provides a valuable and physically sound tool to evaluate the hydrogeomorphological diversities in relation to biodiversity and functions within such assessments.

Conclusions

The importance of hydrogeomorphological heterogeneity for biodiversity and functional diversity in running waters has been repeatedly postulated. However, evidence has been limited to particular spatial and temporal scales of habitat heterogeneity and metrics for habitat heterogeneity are often descriptive (river bed form, substratum type, slope, etc.) rather than rooted in physical principles. Here, we describe a novel diversity framework based on variance partitioning of hydrogeomorphological variations and relate this to biodiversity and ecosystem functioning across different spatio-temporal scales. The framework is routed in basic hydraulic and morphodynamic research but provides significant drivers for biological processes such as the importance of hydrogeomorphological β diversity quantified as the spatial variance of the time-averaged flow velocities and mean water depths.

Our framework is established and tested for microbial communities, but its universal formulation makes it applicable to other organisms. It is transferable to other freshwater ecosystems and ecosystem compartments such as lotic environments and the hyporheic zone, and may include further environmental factors, such as temperature and light.

Hydrogeomorphological simplifications of running waters have reduced the complexity and integrity of riverine ecosystems[70], reducing their biodiversity[71] and functioning[72]. Conservation of biodiversity and the services provided by the operational ecosystems is one of the most important challenges we face as a society. Our framework facilitates integrative studies on the interactions of biotic, functional and hydrogeomorphological diversity and will thus ultimately lead to a broadened diversity concept in stream ecology based on an improved knowledge on how biodiversity–functioning relationships are driven by hydrogeomorphological diversity.

Methods

Study sites

The measurements were conducted at two second-order, gravel-bed mountain streams (Selke, N 51°41'11.5'', E 10°15'34'', Kalte Bode, N 51°44'33'', E 10°42'09'') in Central Germany. Daily discharge data from 1921 (Selke) and 1951 (Kalte Bode) and discharge at 15 min intervals for more recent periods were available from gauging stations close to the study sites. Long-term mean discharge was 1.52 $m^3 s^{-1}$, and 0.72 $m^3 s^{-1}$ and baseflow was 0.24 $m^3 s^{-1}$ and 0.18 $m^3 s^{-1}$ for Selke and Kalte Bode, respectively. The mean widths of the reaches were almost identical for both streams (7.2 m at the Kalte Bode and 7.3 m at the Selke), whereas the mean water level slope of the study reach at the Kalte Bode (0.82 %) was twice as high as at Selke (0.39 %). The length of the study reaches was 588 m (Kalte Bode) and 510 m (Selke), and both reaches were composed of riffle and pool sections with a mean length of 57 ± 56 m (mean ± standard deviation). Assuming that the 84th percentile of a grain size distribution (d_{84}) is a factor of 3.5 larger than the standard deviation of streambed elevations k[73,74] (see Fig. S1 in the Supplement), the relative roughness at the study reaches (d_{84} < water depth > -1 ≈ 0.3) is at the upper end of the typical range of pool-riffle streams[75].

Soluble reactive phosphorous (SRP) and dissolved inorganic nitrogen (DIN, sum of nitrate, ammonium) concentrations were ≤0.003 mg SRP L^{-1} and 0.42-0.91 mg DIN L^{-1} at Kalte Bode and 0.01-0.06 mg SRP L^{-1} and 0.55-1.72 mg DIN L^{-1} at Selke. In comparison, stream water SRP and DIN concentrations were up to 3 to 16 times and up to 2 times higher in the Selke compared to the Kalte Bode, respectively.

Sampling strategy

We established and applied a novel framework for describing diversities using an extensive data set, including flow velocity[16,22,53], streambed topography (measurements new to this study), microbial guilds of biofilms[16], and biofilm nitrogen uptake[53,54]. The adopted

data are based on measurements that were conducted simultaneously at identical spatial scales, except for biofilm diversity and nitrogen uptake, which were sampled in close vicinity but not at the same spot. Data were collected during five sampling campaigns conducted in two mountainous streams with contrasting nutrient backgrounds, respectively and covering two different seasons.

Flow velocity, including turbulent velocity fluctuations, was measured at 533 sampling spots with an acoustic Doppler velocimeter (Vectrino Profiler, Nortek AS, Norway)[16,22,53]. To ensure best-quality data, all measurements were conducted at the so-called sweet spot of the instrument's profiling range[76,77], which was located about 2.3 cm above the streambed in all measurements. At each sampling spot (10^{-2} m), flow velocity was measured for 20 min with a sampling frequency of 64 Hz. Streambed topography was mapped at approximately 1x1 m patches along the stream reaches during four campaigns (in total 58 patches) to analyze geomorphological diversity (further details below).

For three out of the five field campaigns, the diversity of three microbial guilds of epilithic biofilms, namely bacteria, autotrophs and phagotrophic protists was expressed as species or genotype richness at a subset of flow sampling spots[16]. The biofilm was mechanically removed by brushing and rinsing the stone's surface twice with a clean tooth brush and suspended in 30 mL sterile filtered stream water (pore size 0.2 μm). The biofilm suspension was homogenized by ultrasonic treatment, and subsamples were prepared for terminal restriction fragment length polymorphism (T-RFLP) and microscopic observations. General shifts in bacterial diversity were analyzed using 16S rRNA gene-based T-RFLP. The diversity of autotrophs and phagotrophic protists was estimated by microscopic analyses of subsamples. Cyanobacteria and green algae were grouped according to their cell morphology traits in coccoid, comma-like, colonial, and filamentous morphotypes. Diatoms were identified to the level of genera[78]. Heterotrophic protists were identified alive to the lowest

possible taxonomic level; ciliates and testate amoeba were identified to the genus or species level[79–81], flagellates to class or family level[82], and naked amoeba were grouped according to their morphotype[83].

Finally, two field campaigns included measurements of biofilm nitrogen uptake at a subset of flow sampling spots upon adding a ^{15}N labeled (99% enriched) ammonium chloride and bromide as a conservative tracer for 24 h[53]. The tracer injection was 250 m (Kalte Bode) and 136 m and 166 m (Selke summer and spring, respectively) upstream of the study reaches to ensure complete lateral and vertical mixing[84]. Areal nitrogen uptake rates and uptake efficiencies (nitrogen uptake rates normalized by nitrogen biomass) were calculated based on measured ^{15}N enrichment in biofilm samples determined with mass spectrometry.

The data from individual spots were pooled according to two distinct spatial scales: the meso scale (spatial extent of hydrogeomorphological habitats, i.e., riffle and pool, in total 8 riffles and 9 pools), and the reach scale (spatial extent of each of the two study reaches). There were at least three spots pooled for larger scales, and we calculated diversities for each season and stream, except for geomorphological diversities. The streambed surface was stable, and we expected a near bank-full threshold for sediment movement, which was not observed during and between the samplings. We thus pooled the measurements from all seasons to estimate geomorphological diversities at the meso and at the reach scale for each stream (Fig. 1 and Fig. S2 in the Supplement).

Geomorphological measurements and data analysis

Streambed roughness at the spot scale

The streambed topography was surveyed with a custom-made laser scanner[7,85]. A line laser (Z40M18S-F-643-LP60-V2, Z-Laser, Freiburg, Germany) was used to illuminate the streambed, and the reflected light was observed by two underwater cameras (GoPro Hero3+ Black Edition, 48 fps, 1920 x 1440 px). The bottom elevation along the laser line was

reconstructed from the location of the laser line in the calibrated field of view of the cameras. Laser and cameras were mounted on a rack (Fig. S9a), which could be moved horizontally at an adjustable height above the bottom. The rack was mounted on a rigid frame deployed at each patch. After leveling the instrument frame, the laser light sheet was moved along several lanes to scan the streambed topography within an area of 0.8 m x 0.6 m. During laser deployment, the frame was covered with opaque fabric to improve the visibility of the reflected laser line on the bed. The method was restricted to water depths > 10 cm; thus, very shallow areas located mostly near the banks and areas with emerging stones could not be surveyed (< 10% of the wetted width). Individual streambed elevation profiles were merged into a digital elevation model (DEM) of the scanned area with a final horizontal resolution of 0.25 cm (Fig. S9b-c). Although the measurements were obtained at a higher resolution (on average 0.01 cm), we limited the DEM resolution to reduce computational processing time. Data gaps in the DEMs (resulting from, e.g., non-overlapping parts of lanes) were filled using a radial multiquadratic function[86]. Streambed roughness *k* was estimated as the standard deviation of the streambed elevation relative to a planar surface, which we fitted to the observed DEM at each patch. *k* is equivalent to a characteristic vertical roughness height of gravel beds[87]. For each DEM, the distance to the water surface was added to the elevation recorded by the scan.

Streambed roughness at the reach scale and beyond

For spatial extrapolation, longitudinal transects of streambed roughness and water depth were obtained using a remotely controlled laser scan boat (LaSBo)[7]. LaSBo measurements are based on the same laser triangulation method described above but provide longitudinal transects of water depths along the boat trajectory. We measured three longitudinal transects along one riffle (16 m) and two pools (64 m and 68 m) at Selke. The longitudinal transects

were interpolated to a regular spacing of 0.25 cm to match the resolution of the DEMs. Also, LaSBo operation was restricted to water depths > 10 cm.

Topographical data for a 13 km long stream section comprising the investigated study site at Selke were available from the local water authority (i.e., 187 geo-referenced cross-sectional surveys conducted at a daily mean discharge of 0.26 ± 0.08 $m^3 s^{-1}$ (mean ± standard deviation)). The distance between the surveyed cross-sections was 70 ± 28 m (mean ± standard deviation), and we interpolated the cross-sectional mean water depths to a regular spacing of 70 m using the nearest neighbor.

Expression of diversities

Flow and geomorphological diversity

The flow α diversity (α_{flow}) at each spot was calculated as the temporal variance in the longitudinal (u), the transversal (v) and vertical (w) components of the measured flow velocity normalized by the square of the mean flow velocity:

$$\alpha_{\text{flow}} = \frac{1}{\bar{u}^2}\frac{1}{N}\sum_{i=1}^{N}((u_i - \bar{u})^2 + v_i^2 + w_i^2), \quad (1)$$

where $\bar{u} = \frac{1}{N}\sum_{i=1}^{N} u_i$ denotes the mean longitudinal flow velocity and N the number of samples in the velocity time series measured at each spot (note that the mean values of the transversal and vertical velocity components are zero ($\bar{v} = \bar{w} = 0$) after alignment of the measured velocities with the mean flow direction).

Flow γ diversity (γ_{flow}) was calculated by concatenating velocity time series measured at individual spots at the meso or the reach scale for each measurement campaign as:

$$\gamma_{\text{flow}} = \frac{1}{\langle\bar{u}\rangle^2}\frac{1}{n}\sum_{j=1}^{n}\frac{1}{N}\sum_{i=1}^{N}\left(\left(u_{ij} - \langle\bar{u}\rangle\right)^2 + v_{ij}^2 + w_{ij}^2\right), \quad (2)$$

523 with $\langle\bar{u}\rangle$ representing the temporally and spatially averaged flow velocities from *n* different
524 sampling spots within the respective spatial scale ($\langle\bar{u}\rangle = \frac{1}{n}\sum_{j=1}^{n}\frac{1}{N}\sum_{i=1}^{N}u_{ij}$). A minimum
525 number of three velocity measurements was chosen to calculate flow γ diversities at each
526 spatial scale.

527 Finally, β diversity describes the spatial variability obtained from the additive definition of
528 diversities ($\beta = \gamma - \alpha$). Beta flow diversity (β_{flow}) at the meso and reach scale were calculated
529 as:

530 $$\beta_{\text{flow}} = \gamma_{\text{flow}} - \langle\alpha_{\text{flow}}\rangle, \quad (3)$$

531 with $\langle\alpha_{\text{flow}}\rangle$ representing the mean value of all flow α diversities observed at the
532 corresponding scale (see Table 1).

533 While flow diversities were calculated at all spatial scales based on pooled flow
534 velocity measurements at the spot scale, geomorphological diversities were handled slightly
535 differently. The geomorphological α diversity (α_{morpho}) was calculated as the variance of
536 water depth *h* normalized by the square of the mean depth at each patch:

537 $$\alpha_{\text{morpho}} = \frac{1}{\langle h\rangle^2}\frac{1}{N}\sum_{i=1}^{N}\left(h_{ij} - \langle h\rangle\right)^2, \quad (4)$$

538 where $\langle h\rangle = \frac{1}{N}\sum_{i=1}^{N}h_i$ denotes the mean water depth and *N* the number of grid points in the
539 DEM for each patch. γ_{morpho} diversity at the meso and reach scale was calculated by
540 combining all DEMs within the respective spatial scale as:

541 $$\gamma_{\text{morpho}} = \frac{1}{\langle\langle h\rangle\rangle^2}\frac{1}{n}\sum_{j=1}^{n}\frac{1}{N}\sum_{i=1}^{N}\left(\left(h_{ij} - \langle\langle h\rangle\rangle\right)^2\right), \quad (5)$$

542 with $\langle\langle h\rangle\rangle$ representing the spatially averaged mean water depth from *n* patches ($\langle\langle h\rangle\rangle =$
543 $\frac{1}{n}\sum_{j=1}^{n}\frac{1}{N}\sum_{i=1}^{N}h_{ij}$.

544 β_{morpho} for the meso and reach scale was calculated from:

$$\beta_{\mathrm{morpho}} = \gamma_{\mathrm{morpho}} - \langle \alpha_{\mathrm{morpho}} \rangle, \quad (6)$$

with $\langle \alpha_{\mathrm{morpho}} \rangle$ representing the mean values of all α_{morpho} observed at the corresponding scale (see also Table 1).

Table 1. Overview of the α, β and γ components of hydrogeomorphological diversity according to the proposed framework based on variance partitioning of flow velocity and streambed geomorphology at different spatial scales. Angular brackets refer to the overall spatial mean values at the corresponding scale.

Scale	Diver-sity	Flow velocity	Physical description	Streambed geomorphology	Physical description
Spot	α	Temporal flow variability	Temporal variance of flow velocity normalized by the square of its temporal mean (turbulence intensity squared)	Streambed roughness	Spatial variance of water depths normalized by the square of the mean water depth (square of the relative streambed roughness)
Meso, Reach	β	Spatial flow variability	Spatial variance of time-averaged flow velocities normalized by the square of overall mean velocity	(Mean) Water depth variability	Spatial variance of the mean water depths at the spot scale normalized by the square of their overall mean
	γ	Overall flow diversity	Total temporal and spatial variance of flow velocity normalized by the square of their overall mean ($\gamma = <\alpha> + \beta$)	Overall geomorphological diversity	Total spatial variance of water depths normalized by the square of their overall mean ($\gamma = <\alpha> + \beta$)

Temporal and spatial upscaling

For the Selke, power spectral densities of the longitudinal velocity component were estimated for each 20-min measurement using Welch's method[88] with 50% overlap and a Hamming window function. Spectra were normalized by the square of the mean flow velocity. The normalized velocity spectra represent the frequency distribution of components of the flow α diversity (see also equation (1)). The individual spectra from the 20-min flow measurements were log-averaged, and the mean spectrum and the 5% and 95% percentiles were calculated. Next, we constructed a composite spectrum of velocity fluctuations by

557 combining: (1) the log-averaged spectra and their percentiles (frequency range from $3x10^{1}$ to
558 $4x10^{-3}$ Hz); (2) the spectra of the mean velocities calculated from 15 min interval discharge
559 data for three months (frequency from $5x10^{-4}$ to $1x10^{-7}$ Hz); and (3) the mean velocities
560 calculated from daily mean discharge data for 16 years (frequency from $6x10^{-6}$ to $3x10^{-9}$ Hz).
561 The discharge data were converted to flow velocities using a cross-sectional topographic
562 transect and water level data at the gauging station. The cumulative α diversity for increasing
563 time scales was estimated as the cumulative integral of the composite spectral density from
564 the highest to lowest resolved frequency, i.e., the cumulative variance for increasing time
565 scales.

566 Similar to flow velocity, a composite power spectrum of water depth variations was
567 estimated by combining the wavenumber spectra of (1) all concatenated LaSBo surveys at the
568 Selke (wavenumber from $2x10^{2}$ to 10^{-2} m^{-1}) and (2) cross-sectional mean water depths
569 calculated from the 13 km survey at the Selke (wavenumber from $7x10^{-3}$ to $1x10^{-4}$ m^{-1}). All
570 spectra were normalized by the corresponding squared mean water depth. The cumulative,
571 normalized variance for increasing length scales was estimated as cumulative integrals of the
572 spectral density function from high to low frequencies. The unresolved wave number range
573 from $7x10^{-3}$ to 10^{-2} m^{-1} was linearly interpolated for integration.

574 Diversity of microbial guilds

575 α diversity of microbial guilds, namely bacteria, autotrophs and phagotrophic protists,
576 were represented by species richness at the spot scale[16]. At larger spatial scales, the mean α
577 diversity of all spots within a pre-defined scale (meso or reach scale) was calculated. In
578 addition, γ diversity at the meso and reach scale was calculated by considering all species
579 found at the respective spatial scale. The difference between γ and mean α diversity
580 represents β diversity, by adopting the additive definition of diversities. At the meso scale, we

calculated diversities for riffles and pools separately for each season and stream resulting in mean α, β, and γ diversities for riffles and mean α, β, and γ diversities for pools.

Diversity of biofilm nitrogen uptake

Similar to geomorphological diversity, the variance of spot-scale nitrogen uptake rates and nitrogen uptake efficiencies within each riffle or pool normalized by the mean square was the α component of uptake diversities (coefficient of variation, CV). To calculate mean α diversities at the meso scale, we followed a similar approach as for biofilms averaging all riffle and all pool α diversities separately for each campaign, resulting in a mean α diversity for riffles and a mean α diversity for pools. Next, we calculated the CV for all spots in all riffles and for all spots in all pools along the stream reach for each campaign as γ diversities: γ (meso scale) $_{\text{riffle}}$ is the CV of uptake rates and efficiencies in riffle spots, and γ (meso scale) $_{\text{pool}}$ is the CV of uptake in pool spots along the reach. The β diversity of uptake in riffles and pools was obtained by subtracting the mean α diversity from the corresponding γ diversity for each campaign. At the reach scale, we calculated the mean α diversity of uptake from all meso-scale α diversities for each campaign and the γ diversity as the CV across all spots within the reach. Finally, we subtracted the mean α diversity from the γ diversity to achieve the β diversity at the reach scale.

Statistical analyses

We were interested in identifying whether each of the three components of flow diversity (α, β and γ) was a significant predictor of the corresponding diversity component of geomorphology, microbial guilds, nitrogen uptake rate and nitrogen uptake efficiency at identical scales. We expected a linear relationship within the range of diversities observed and used a linear regression model with a fixed effect intercept to examine the relationship between the predictor variable flow mean α diversity and the response variable

geomorphological mean α diversity. For each model, data from both streams, all scales and seasons were used, and we included stream and season as additional explanatory variables as we expected that differences in ambient environmental factors associated with stream or season explained a part of the variation in the response variable. Stream and season were added to the model without an interaction term. We refrained from testing for differences between meso- and reach scale because we only sampled one reach per stream. Data were log-transformed if residuals were not normally distributed (Shapiro-Wilk Test). All test results were regarded as significant if $p < 0.05$.

Furthermore, we tested for significant relationships between biodiversity and ecosystem functioning. We tested whether the three components of microbial diversity (α, β and γ) were significantly related to the corresponding diversity component of nitrogen uptake rate and uptake efficiency, as well as to the mean total nitrogen uptake rate and uptake efficiency. Linear regression models were fitted to the data as described above. All tests were performed in Matlab (version R2019b; MathWorks, Natick, Massachusetts) using the 'fitlm' function.

Data Availability

The data that support the findings of this study are available from the corresponding author upon reasonable request.

Acknowledgments

The research was supported by the German Science Foundation (DFG, grant numbers LO 1150/8-1 and WE 3545/6-1), the 2020-2021 Biodiversa+ and Water JPI joint call for research projects, under the BiodivRestore ERA-NET Cofund (GA N°101003777), with the EU and the funding organizations Federal Ministry of Education and Research Germany

(grant numbers: 16LW0175, 16LW0174K) and the Agencia Estatal De Investigación (AEI), Spain. U.R.-B. was supported by the Carl Zeiss Foundation (excellence grant P2021-00-004). We are grateful to P. Portius and his team for technical support and construction of the frame for the laser scanner, S. Bauth, M. Diener, N. Oberhoffner, C. Mendoza-Lera, K. Kalla and M. Vieweg for field assistance. We appreciate valuable comments from Antonis Chatzinotas on previous drafts of the manuscript, and we thank the „Landesbetrieb für Hochwasserschutz und Wasserwirtschaft“ (LHW) Sachsen-Anhalt for providing data on the streams. The authors declare no conflict of interest.

References

1. O'Neill, R. V, Gardner, R. H., Milne, B. T., Turner, M. G. & Jackson, B. Heterogeneity and Spatial Hierarchies. in *Ecological Heterogeneity* (eds. Kolasa, J. & Pickett, S. T. A.) 85–96 (Springer New York, 1991). doi:10.1007/978-1-4612-3062-5_5

2. Palmer, M. A., Hakenkamp, C. C. & Nelson-Baker, K. Ecological Heterogeneity in Streams : Why Variance Matters. *J. North Am. Benthol. Soc.* **16**, 189–202 (1997).

3. Tews, J. *et al.* Animal species diversity driven by habitat heterogeneity/diversity: the importance of keystone structures. *J. Biogeogr.* **31**, 79–92 (2004).

4. Wilcox, K. R. *et al.* Asynchrony among local communities stabilises ecosystem function of metacommunities. *Ecol. Lett.* **20**, 1534–1545 (2017).

5. Nikora, V. Hydrodynamics of aquatic ecosystems: An interface between ecology, biomechanics and environmental fluid mechanics. *River Res. Appl.* **26**, 367–384 (2010).

6. Biggs, B. J. F., Nikora, V. & Snelder, T. H. Linking scales of flow variability to lotic ecosystem structure and function. *River Res. Appl.* **21**, 283–298 (2005).

7. Noss, C. & Lorke, A. Roughness, resistance, and dispersion: Relationships in small streams. *Water Resour. Res.* **52**, 2802–2821 (2016).

8. Lamarre, H. & Roy, A. G. Reach scale variability of turbulent flow characteristics in a gravel-bed river. *Geomorphology* **68**, 95–113 (2005).

9. Frissell, C. A., Liss, W. J., Warren, C. E. & Hurley, M. D. A Hierarchical Framework for Stream Habitat Classification : Viewing Streams in a Watershed Context. *Environ. Manag.* **10**, 199–214 (1986).

10. Zavadil, E. & Stewardson, M. The Role of Geomorphology and Hydrology in Determining Spatial-Scale Units for Ecohydraulics. in *Ecohydraulics: An Integrated Approach* (eds. Maddock, I., Harby, A., Kemp, P. & Wood, P. J.) 125–142 (John Wiley and Sons, 2013).

11. Gostner, W., Alp, M., Schleiss, A. J. & Robinson, C. T. The hydro-morphological index of diversity: a tool for describing habitat heterogeneity in river engineering projects. *Hydrobiologia* **712**, 43–60 (2013).

12. Statzner, B., Gore, J. A. & Resh, V. H. Hydraulic Stream Ecology: Observed Patterns and Potential Applications. *J. North Am. Benthol. Soc.* **7**, 307–360 (1988).

13. Vogel, S. *Life in Moving Fluids*. (Princeton University Press, 1983). doi:10.1515/9780691212975

14. Hart, D. D. & Finelli, C. M. Physical-Biological Coupling in Streams: The Pervasive Effects of Flow on Benthic Organisms. *Annu. Rev. Ecol. Syst.* **30**, 363–395 (1999).

15. Wohl, E. Spatial heterogeneity as a component of river geomorphic complexity. *Prog. Phys. Geogr.* **40**, 598–615 (2016).

16. Risse-Buhl, U. *et al.* Near streambed flow shapes microbial guilds within and across trophic levels in fluvial biofilms. *Limnol. Oceanogr.* **65**, 2261–2277 (2020).

17. Besemer, K., Singer, G. A., Hödl, I. & Battin, T. J. Bacterial community composition of stream biofilms in spatially variable-flow environments. *Appl. Environ. Microbiol.* **75**, 7189–7195 (2009).

18. Peipoch, M. *et al.* Small-scale heterogeneity of microbial N uptake in streams and its implications at the ecosystem level. *Ecology* **97**, 1329–1344 (2016).

19. Palmer, M. A., Menninger, H. L. & Bernhardt, E. S. River restoration, habitat heterogeneity and biodiversity: a failure of theory or practice? *Freshw. Biol.* **55**, 205–

222 (2010).

20. Barton, P. S. *et al.* The spatial scaling of beta diversity. *Glob. Ecol. Biogeogr.* **22**, 639–647 (2013).

21. Singer, G. A., Besemer, K., Schmitt-Kopplin, P., Hodl, I. & Battin, T. J. Physical heterogeneity increases biofilm resource use and its molecular diversity in stream mesocosms. *PLoS One* **5**, (2010).

22. Risse-Buhl, U. *et al.* The role of hydrodynamics in shaping the composition and architecture of epilithic biofilms in fluvial ecosystems. *Water Res.* **127**, 211–222 (2017).

23. Palmer, M. & Ruhi, A. Linkages between flow regime, biota, and ecosystem processes: Implications for river restoration. *Science (80-.).* **365**, eaaw2087 (2019).

24. Lepori, F., Palm, D., Brännäs, E. & Malmqvist, B. Does restoration of structural heterogeneity in streams enhance fish and macroinvertebrate diversity? *Ecol. Appl.* **15**, 2060–2071 (2005).

25. Moellering, H. & Tobler, W. Geographical variances. *Geogr. Anal.* **4**, 34–50 (1972).

26. Wu, J., Jelinski, D. E., Luck, M. & Tueller, P. T. Multiscale Analysis of Landscape Heterogeneity: Scale Variance and Pattern Metrics. *Ann. GIS* **6**, 6–19 (2000).

27. Ward, J. V & Tockner, K. Biodiversity: Towards a unifying theme for river ecology. *Freshw. Biol.* **46**, 807–819 (2001).

28. Li, Y. *et al.* Modeling the Effects of Hydrodynamic Regimes on Microbial Communities within Fluvial Biofilms: Combining Deterministic and Stochastic Processes. *Environ. Sci. Technol.* **49**, 12869–12878 (2015).

29. Weitere, M. *et al.* The food web perspective on aquatic biofilms. *Ecol. Monogr.* **88**, 543–559 (2018).

30. Whittaker, R. H. Evolution and Measurement of Species Diversity. *Taxon* **21**, 213 (1972).

31. Whittaker, R. H. Vegetation of the Siskiyou Mountains, Oregon and California. *Ecol. Monogr.* **30**, 279–338 (1960).

32. Jost, L. Partitioning diversity into independent alpha and beta components. *Ecology* **88**, 2427–2439 (2007).

33. Anderson, M. J. *et al.* Navigating the multiple meanings of β diversity: a roadmap for the practicing ecologist. *Ecol. Lett.* **14**, 19–28 (2011).

34. Nikora, V. Hydrodynamics of gravel-bed rivers: scale issues. in *Gravel-Bed Rivers VI: From Process Understanding to River Restoration* (eds. Habersack, H., Piégay, H. & Rinaldi, M.) 61–81 (Elsevier B.V.: Amsterdam, The Netherlands, 2008). doi:10.1016/S0928-2025(07)11113-5

35. Palmer, M. A. & Poff, N. L. The Influence of Environmental Heterogeneity on Patterns and Processes in Streams. *J. North Am. Benthol. Soc.* **16**, 169–173 (1997).

36. Thorp, J. H., Thoms, M. C. & Delong, M. D. The riverine ecosystem synthesis: Biocomplexity in river networks across space and time. *River Res. Appl.* **22**, 123–147 (2006).

37. Roy, A. G., Buffin-Bélanger, T., Lamarre, H. & Kirkbride, A. D. Size, shape and dynamics of large-scale turbulent flow structures in a gravel-bed river. *J. Fluid Mech.* **500**, 1–27 (2004).

38. Hauer, C., Unfer, G., Tritthart, M., Formann, E. & Habersack, H. Variability of mesohabitat characteristics in riffle-pool reaches: Testing an integrative evaluation concept (FGC) for MEM-application. *River Res. Appl.* **27**, 403–430 (2011).

39. Parasiewicz, P. The MesoHABSIM model revisited. *River Res. Appl.* **23**, 893–903

(2007).

40. Smith, M. W. Roughness in the Earth Sciences. *Earth-Science Rev.* **136**, 202–225 (2014).

41. Aberle, J. & Smart, G. The influence of roughness structure on flow resistance on steep slopes. *J. Hydraul. Res.* **41**, 259–269 (2003).

42. Nikora, V. *et al.* Double-averaging concept for rough-bed open-channel and overland flows: Theoretical background. *J. Hydraul. Eng.* **133**, 873–883 (2007).

43. Cooper, J. R. & Tait, S. J. The spatial organisation of time-averaged streamwise velocity and its correlation with the surface topography of water-worked gravel beds. *Acta Geophys.* **56**, (2008).

44. Cooper, J. R. & Tait, S. J. Water-worked gravel beds in laboratory flumes - a natural analogue? *Earth Surf. Process. Landforms* **34**, 384–397 (2009).

45. Reid, M. A. & Thoms, M. C. Surface flow types, near-bed hydraulics and the distribution of stream macroinvertebrates. *Biogeosciences* **5**, 1043–1055 (2008).

46. Blanckaert, K., Garcia, X.-F., Ricardo, A. M., Chen, Q. & Pusch, M. T. The role of turbulence in the hydraulic environment of benthic invertebrates. *Ecohydrology* **6**, 700–712 (2013).

47. Vannote, R. L., Minshall, G. W., Cummins, K. W., Sedell, J. R. & Cushing, C. E. River Continuum Concept. *Can. J. Fish. Aquat. Sci.* **37**, 130–137 (1980).

48. Huisman, J. *et al.* Cyanobacterial blooms. *Nat. Rev. Microbiol.* **16**, 471–483 (2018).

49. Wu, X., Noss, C., Liu, L. & Lorke, A. Effects of small-scale turbulence at the air-water interface on microcystis surface scum formation. *Water Res.* **167**, 115091 (2019).

50. Olden, J. D. & Naiman, R. J. Incorporating thermal regimes into environmental flows

753 assessments: modifying dam operations to restore freshwater ecosystem integrity.
754 *Freshw. Biol.* **55**, 86–107 (2010).

755 51. Cooper, M. *et al.* Recent advances in stream and river temperature research. *Hydrol.*
756 *Process.* **22**, 902–918 (2008).

757 52. Harrigan, K. M. & Moore, P. A. Scaling to the Organism: An Innovative Model of
758 Dynamic Exposure Hotspots in Stream Systems. *Arch. Environ. Contam. Toxicol.*
759 (2017). doi:10.1007/s00244-017-0444-3

760 53. Anlanger, C. *et al.* Hydraulic and biological controls of biofilm nitrogen uptake in
761 gravel-bed streams. *Limnol. Oceanogr.* **66**, 3887–3900 (2021).

762 54. Risse-Buhl, U. *et al.* Hydromorphologic Sorting of In-Stream Nitrogen Uptake Across
763 Spatial Scales. *Ecosystems* **24**, 1184–1202 (2021).

764 55. Powell, D. M. Flow resistance in gravel-bed rivers: Progress in research. *Earth-Science*
765 *Rev.* **136**, 301–338 (2014).

766 56. Terui, A., Kim, S., Dolph, C. L., Kadoya, T. & Miyazaki, Y. Emergent dual scaling of
767 riverine biodiversity. *Proc. Natl. Acad. Sci. U. S. A.* **118**, (2021).

768 57. Besemer, K. *et al.* Biophysical controls on community succession in stream biofilms.
769 *Appl. Environ. Microbiol.* **73**, 4966–4974 (2007).

770 58. Willkomm, M., Schlussel, A., Reiz, E. & Arndt, H. Effects of microcurrents in the
771 boundary layer on the attachment of benthic heterotrophic nanoflagellates. *Aquat.*
772 *Microb. Ecol.* **48**, 169 (2007).

773 59. Risse-Buhl, U. *et al.* Detachment and motility of surface-associated ciliates at increased
774 flow velocities. *Aquat. Microb. Ecol.* **55**, 209–218 (2009).

775 60. Cardinale, B. J. Biodiversity improves water quality through niche partitioning. *Nature*

472, 86–89 (2011).

61. Chew, S. C. *et al.* Dynamic Remodeling of Microbial Biofilms by Functionally Distinct Exopolysaccharides. *MBio* **5**, 1–11 (2014).

62. Hou, J., Veeregowda, D. H., van de Belt-Gritter, B., Busscher, H. J. & van der Mei, H. C. Extracellular Polymeric Matrix Production and Relaxation under Fluid Shear and Mechanical Pressure in Staphylococcus aureus Biofilms. *Appl. Environ. Microbiol.* **84**, 1–14 (2018).

63. Hall-Stoodley, L., Costerton, J. W. & Stoodley, P. Bacterial biofilms: from the Natural environment to infectious diseases. *Nat. Rev. Microbiol.* **2**, 95–108 (2004).

64. Grant, S. B., Azizian, M., Cook, P., Boano, F. & Rippy, M. A. Factoring stream turbulence into global assessments of nitrogen pollution. *Science (80-.).* **359**, 1266–1269 (2018).

65. Wild, R., Gücker, B., Weitere, M. & Brauns, M. Resource supply and organismal dominance are associated with high secondary production in temperate agricultural streams. *Funct. Ecol.* **36**, 2367–2383 (2022).

66. Walker, B. H. Biodiversity and Ecological Redundancy. *Conserv. Biol.* **6**, 18–23 (1992).

67. Tuomisto, H. A diversity of beta diversities: straightening up a concept gone awry. Part 1. Defining beta diversity as a function of alpha and gamma diversity. *Ecography (Cop.).* **33**, 2–22 (2010).

68. Stevenson, R. J., Peterson, C. G., Kirschtel, D. B., King, C. C. & Tuchman, N. C. Density-dependent growth, ecological strategies, and effects of nutrients and shading on benthic diatom succession in streams. *J. Phycol.* **27**, 59–69 (1991).

69. Vörösmarty, C. J. *et al.* Global threats to human water security and river biodiversity.

Nature **467**, 555–561 (2010).

70. Peipoch, M., Brauns, M., Hauer, F. R., Weitere, M. & Valett, H. M. Ecological Simplification: Human Influences on Riverscape Complexity. *Bioscience* **65**, 1057–1065 (2015).

71. Albert, J. S. *et al.* Scientists' warning to humanity on the freshwater biodiversity crisis. *Ambio* **50**, 85–94 (2021).

72. Brauns, M. *et al.* A global synthesis of human impacts on the multifunctionality of streams and rivers. *Glob. Chang. Biol.* 1–11 (2022). doi:10.1111/gcb.16210

73. Aberle, J. & Nikora, V. Statistical properties of armored gravel bed surfaces. *Water Resour. Res.* **42**, (2006).

74. Heritage, G. L. & Milan, D. J. Terrestrial Laser Scanning of grain roughness in a gravel-bed river. *Geomorphology* **113**, 4–11 (2009).

75. Wohl, E. & Merritt, D. M. Reach-scale channel geometry of mountain streams. *Geomorphology* **93**, 168–185 (2008).

76. Koca, K., Noss, C., Anlanger, C., Brand, A. & Lorke, A. Performance of the Vectrino Profiler at the sediment–water interface. *J. Hydraul. Res.* **55**, 573–581 (2017).

77. Brand, A., Noss, C., Dinkel, C. & Holzner, M. High-Resolution Measurements of Turbulent Flow Close to the Sediment–Water Interface Using a Bistatic Acoustic Profiler. *J. Atmos. Ocean. Technol.* **33**, 769–788 (2016).

78. Cox, E. J. *Identification of Freshwater Diatoms from Live Material*. (Chapman & Hall, 1996).

79. Page, F. C. & Siemensma, F. J. *Nackte Rhizopoden und Heliozoea*. (Gustav Fischer Verlag, 1991).

80. Foissner, W. & Berger, H. A user-friendly guide to the ciliates (Protozoa, Ciliophora) commonly used by hydrobiologists as bioindicators in rivers, lakes, and waste waters, with notes on their ecology. *Freshw. Biol.* **35**, 375–482 (1996).

81. Patterson, D. J. *Freeliving Freshwater Protozoa*. (John Wiley and Sons Publishing, 1996).

82. Jeuck, A. & Arndt, H. A Short Guide to Common Heterotrophic Flagellates of Freshwater Habitats Based on the Morphology of Living Organisms. *Protist* **164**, 842–860 (2013).

83. Smirnov, A. V & Goodkov, A. V. An illustrated list of basic morphotypes of Gymnamoebia (Rhizopoda, Lobosea). *Protistology* **1**, 20–29 (1999).

84. Day, T. J. Observed mixing lengths in mountain streams. *J. Hydrol.* **35**, 125–136 (1977).

85. Noss, C., Wilkinson, J. & Lorke, A. Triangulation hand-held laser-scanning (TriHaLaS) for micro- and meso-habitat surveys in streams. *Earth Surf. Process. Landforms* (2018). doi:10.1002/esp.4310

86. Nikora, V. & Walsh, J. Water-worked gravel surfaces: High-order structure functions at the particle scale. *Water Resour. Res.* **40**, 1–7 (2004).

87. Nikora, V., Goring, D. G. & Biggs, B. J. F. On gravel-bed roughness characterization. *Water Resour. Res.* **34**, 517–527 (1998).

88. Welch, P. The use of fast Fourier transform for the estimation of power spectra: A method based on time averaging over short, modified periodograms. *IEEE Trans. Audio Electroacoust.* **15**, 70–73 (1967).